AEROSOL ABSORPTION IN CLOUDY SCENES USING PASSIVE SATELLITE INSTRUMENTS

M. de Graaf, L.G. Tilstra, and P. Stammes

Royal Netherlands Meteorological Institute (KNMI), Wilhelminalaan 10, 3732 GK, De Bilt, The Netherlands

Abstract

A method is presented to determine the energy absorbed by aerosols overlying clouds, using passive remote sensing by satellites. In passive remote sensing techniques, determination of the optical thickness of aerosols is severely hampered by the brightness of clouds in a scene. This makes the study of the various direct and indirect aerosol effects on clouds difficult and passive satellite observations of these effects are often limited to aerosols in the vicinity of clouds. Very valuable information has become available from active space-based sensors and some dedicated field campaigns on aerosol indirect effects have been performed in the past. This new method will exploit the wealth of information from the passive, space-based spectrometer SCIAMACHY that has been obtained over the last 9 years.

Cloud scattering is large in the entire solar spectral range and cloud optical thickness is generally much larger than aerosol optical thickness. Therefore, scattering aerosols cannot, at present, be distinguished from scattering cloud droplets. Cloud absorption, on the other hand, is negligible below about 1 micron, whereas aerosol absorption is largest in the UV wavelength range, and increases with decreasing wavelength. A frequently used satellite tool to detect absorbing aerosols, which uses this aerosol UV-absorption, is the Absorbing Aerosol Index (AAI), which can indicate absorbing aerosols overlying clouds. The AAI is available from SCIAMACHY and used to find aerosol-polluted cloud scenes. A quantitative measure of absorption by aerosols, like e.g. aerosol optical thickness and aerosol scattering albedo, has been proved hard to derive from the AAI, which is a radiation property and not an aerosol property. Therefore, in the method presented here, the radiation, or reflectance as measured by SCIAMACHY, is used directly to derive the absorbed energy by the aerosols in the UV and visible spectral range, without making any assumptions on the aerosol microphysical properties. A LookUp Table (LUT) of cloud reflectances was created, simulating the spectral reflectances in the UV and visible range of aerosol-free cloud scenes. From an actual, measured aerosol-polluted cloud scene the cloud optical thickness and cloud droplet size are determined at wavelengths above 1 micron, to minimise any aerosol effect on the cloud properties. These cloud properties are then used with the predetermined LUT to get the simulated aerosol-free cloud reflectance in the UV and visible spectral range for the measured scene. The simulated aerosol-free and measured aerosol-polluted spectral reflectances can be compared directly to determine the absorbed energy by aerosols in the scene.

INTRODUCTION

The direct radiative effect of absorbing aerosols in cloudy scenes is currently not well constrained [*Forster et al.*, 2007; *Yu et al.*, 2006]. The simultaneous observation of both clouds and aerosols is seriously limited due to their heterogeneous distribution in space and time. Space-based observations have the potential of monitoring cloud and aerosol distributions on a daily basis, but most current satellite aerosol retrieval algorithms rely on cloud screening before retrieving aerosol information [e.g. *Tanré et al.*, 1996; *Torres et al.*, 1998; *Veefkind et al.*, 2000; *Diner et al.*, 2001; *King*, 2003; *Hauser et al.*, 2005]. Here, we introduce a novel technique to retrieve the aerosol direct effect over clouds, using spectral reflectance observations from space. The UV–visible part of the reflectance spectrum is attenuated due to the light absorption by the small, absorbing aerosols [*De Graaf et al.*, 2007]. This

results in a darkening of the cloud scene in the UV and a positive radiative effect. The infrared part of the reflectance spectrum, however, is not significantly attenuated by aerosol absorption. Therefore, cloud parameters can be retrieved in this part of the spectrum, where the aerosol optical thickness has been reduced to a sufficiently small number. Using the retrieved cloud optical thickness and cloud droplet size, the cloud reflectance spectrum is then modelled using a Radiative Transfer Model (RTM), effectively removing the aerosols from the scene. By comparison of the measured polluted cloud scene and the modelled unpolluted cloud scene, the aerosol direct effect can be estimated directly, without the need for any aerosol parameter estimates. This technique is illustrated here using reflectance spectra from the space-borne spectrometer SCIAMACHY, which measures 92% of the solar energy spectrum reflected by the Earth's atmosphere and surface.

METHODS AND DATA

SCIAMACHY polluted cloud reflectance spectra

Polluted cloud spectra can typically be found from high Absorbing Aerosol Index (AAI) values combined with high cloud fraction values [*Stammes et al.*, 2008, *Wilcox*, 2011]. The SCIAMACHY AAI [*De Graaf and Stammes*, 2005] indicates the presence UV–absorbing aerosols, over both land and ocean, also in cloud-covered scenes as long as the aerosols overlie the cloud [*De Graaf et al.*, 2007]. Cloud fraction and cloud pressure can be retrieved using the updated Fast Retrieval Scheme for Clouds from the Oxygen A–band (FRESCO+) database for SCIAMACHY measurements [*Wang et al.*, 2008]. FRESCO+ retrieves cloud pressure and effective cloud fraction using the O2–A absorption band around 760 nm. FRESCO+ cloud pressure is about the optical midlevel of the cloud. Cloud height retrievals can be significantly perturbed by overlying aerosol layers [*Waquet et al.*, 2009], which is relevant in this study. However, cloud height as retrieved by FRESCO+ was found to be the least affected cloud height parameter from three commonly used space-based algorithms for retrieving cloud height and can be used to fix the modelled cloud height. Furthermore, radiative transfer simulations performed for this study and by others [e.g. *Ahmad et al.*, 2004] show that the TOA reflectance is not affected much by the physical height of the cloud, except for extreme viewing geometries.

Modelled unpolluted cloud reflectance spectra

The simulation of aerosol-free cloud reflectance spectra is based on a database of cloud reflectance spectra, modelled for a wide variety of conditions, using the Doubling-Adding KNMI (DAK) radiative transfer model [*Stammes*, 2001]. DAK computes the vectorized monochromatic reflectance and transmittance of a pseudo-spherical atmosphere, using the polarized doubling-adding method [*De Haan et al.*, 1987]. The internal radiation field of the atmosphere is determined in a finite number of layers, each of which can have Rayleigh scattering, gas absorption, and aerosol and cloud particle scattering and absorption. Using the measured scene geometry, surface albedo and ozone column, the scene cloud optical thickness and cloud droplet size are first retrieved using an inversion scheme. The cloud TOA reflectance at wavelengths below 1.0 µm is mainly determined by the optical thickness of the cloud, while the cloud TOA reflectance above about 2.5 µm is mainly determined by the cloud droplet size [*Nakajima and King*, 1990]. Between these two wavelengths the TOA reflectance carries information of both parameters. This is the basis for retrievals of cloud droplet effective radius and cloud optical thickness using, e.g., Advanced Very High Resolution Radiometer (AVHRR) [*Kawamoto et al.*, 2001], Moderate Resolution Imaging Spectroradiometer (MODIS) [*Platnick et al.*, 2003] and Spinning Enhanced Visible and Infrared Imager (SEVIRI) [*Roebeling et al.*, 2006].

Below about 1.0 µm however, the optical thickness of absorbing aerosols is not negligible in many cases, and the TOA reflectance can be attenuated by aerosol absorption. Consequently, overlying aerosol layers can affect the retrieval of cloud droplet size and cloud optical thickness [*Haywood et al.*, 2004; *Coddington et al.*, 2010]. This effect increases with increasing aerosol (absorbing) optical thickness and is important in the current context. Therefore, the cloud parameters must be retrieved at wavelengths in the near–infrared where the aerosol absorption is sufficiently low. For this study the 1051 and 1640 nm bands were used, which are outside any large gas absorption bands and where the aerosol absorption optical thickness has decreased sufficiently. Using the retrieved cloud parameters from the inversion scheme and FRESCO+ and the scene parameters, the unpolluted

cloud reflectance spectrum for the measured scene can be modelled, effectively removing the aerosols from the scene. To simulate all the fine structured absorption bands in the reflectance spectrum, the SCIAMACHY measured aerosol-polluted cloud spectrum is matched to the simulated spectrum at the simulated wavelengths using a multiplication factor. This factor is linearly interpolated between the simulated wavelengths. This implicitly assumes that the aerosols absorption has no spectral features. In this way a fine structured cloud reflectance spectrum, free from aerosol absorption, is simulated.

RESULTS

In August 2006 a two–week period of high AAI over clouds could be observed over the South-Atlantic Ocean off the west coast of Namibia. These events can often be observed in this area from June to September, which is the local dry season. The high AAI values are caused by smoke from vegetation fires on the African mainland, which are advected over the Atlantic at altitudes of typically 1 – 5 kilometers [e.g. *De Graaf et al.*, 2007].

A typical heterogeneous horizontal distribution of the cloud and aerosol fields off the west coast of Namibia is shown in Figure 1, where SCIAMACHY AAI measurements are overlaid on a MERIS RGB image. The high AAI values are indicative of anomalous absorption in the UV, typically caused by UV–absorbing aerosols, when ozone absorption is accounted for [*Herman et al.*, 1997; *Torres et al.*, 1998; *De Graaf et al.*, 2005]. Clearly, the horizontal distributions of aerosols and clouds are very variable, and change rapidly from day to day. Monitoring of the aerosol direct effect from passive instruments with daily global coverage will be highly advantageous for the understanding of aerosol–cloud interactions. The vertical configuration for the event in Figure 1 is shown using a spatially co-located CALIPSO overpass. The CALIOP 1064 nm backscatter signal shown in Figure 2 was acquired during the daytime, which makes it noisier than the nighttime signal, but it is separated in time only 4 hours from the ENVISAT overpass. It shows the strongly reflecting cloud layer at around 500 m altitude and the vertically extensive smoke layer between about 1 and 4 km altitude.
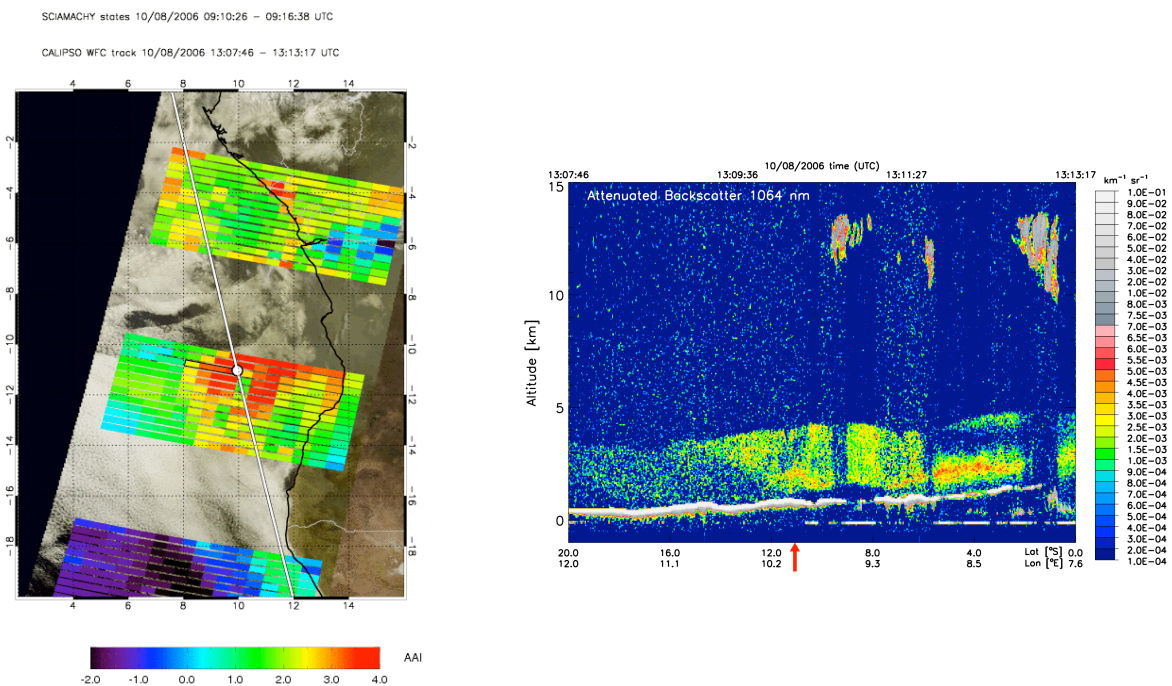

Figure 1: **Horizontal (left) and vertical (right) distribution of clouds and aerosols on 10 August 2006 over the South Atlantic Ocean. In the left image SCIAMACHY AAI values are overlain on a MERIS and NASA Blue marble RGB composite. The CALIPSO track is plotted in white. The attenuated backscatter signal at 1064 nm is plotted in the right image. The red arrow corresponds to the white dot. The reflectance spectrum of the black rectangle in the left image is plotted in Figure 2.**
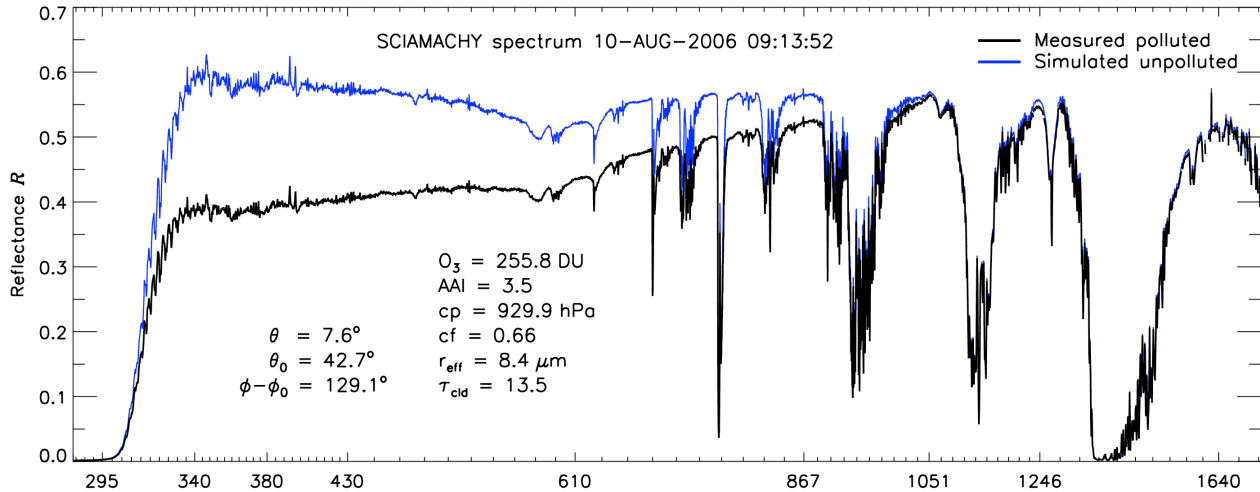
Figure 2: Measured SCIAMACHY spectrum of 10 August 2006 at 09:13:52 UTC (black). The FRESCO+ cloud fraction for this scene was 0.66, with a cloud pressure of 929.9 hPa. The total ozone column was 255.8 DU. The AAI for the entire 1s pixel was 3.5, indicating the reduction of UV radiation due to absorption by aerosols above the clouds. The retrieved cloud droplet size was 8.4 microns, with a cloud optical thickness of 13.5. The simulated cloud reflectance spectrum without aerosols for these cloud and scene parameters is shown in blue.

The red arrow indicates the location of the white dot in Figure 1, where the AAI reaches a high value of about 4.0. Clearly, absorbing aerosols overlie the clouds at this point, causing the high AAI value. This is illustrated by the reflectance spectrum, which is shown in Figure 2 by the black line. The AAI in Figure 1 is given on a 0.25 s integration time resolution, but the complete reflectance spectrum from the UV to IR is only available on a 1 s integration time resolution, so four neighboring pixels must be co-added. Therefore the spectrum in Figure 2 represents the average reflectance spectrum from the four pixels indicated by the black rectangle in Figure 1.

The blue curve in Figure 2 represents the simulated reflectance spectrum for this scene with the aerosol layer removed. The cloud parameters for this simulation where determined from the SCIAMACHY measurements at 1051 and 1640 nm. The retrieved effective cloud droplet size was 8.4 micron, the retrieved cloud optical thickness 13.5, the total ozone column 255.8 DU and the cloud pressure 929.9 hPa. The resulting cloud spectrum deviates from the measured spectrum in the UV, and (by construction) resembles the measured spectrum in the IR.

The energy absorbed by the aerosols is proportional to the difference between the black and the blue curve, shown in Figure 3a. The spectrally resolved aerosol direct radiative effect can be estimated by convolution of the reflectance difference with the solar irradiance spectrum, shown in Figure 3b. The result is shown in Figure 3c. The estimated total aerosol radiative effect of this scene is 73 Wm^{-2}. This is 8% of the total incident solar irradiance, which was 910 Wm^{-2} in the range measured by SCIAMACHY at the current solar elevation angle.

CONCLUSIONS

A new method was introduced to quantify the direct aerosol effect over clouds using space-based spectrometer measurements and radiative transfer model results of cloud scene TOA reflectances. In order to avoid the difficulties in retrieving aerosol parameters from satellite instruments in general, and in cloudy scenes in particular, only cloud parameters are retrieved from the measurements, along with essential scene parameters that are needed to characterize the cloud reflectance spectrum. The latter include generally available parameters like scattering geometry, ozone column density and surface albedo. Cloud fraction and cloud height can be retrieved using well–established retrieval methods. The FRESCO+ algorithm was used here, which was shown to be relatively unaffected by aerosol contamination. Cloud droplet size and cloud optical thickness can be retrieved in the infrared with also well–established algorithms used for MODIS and SEVIRI, among others.
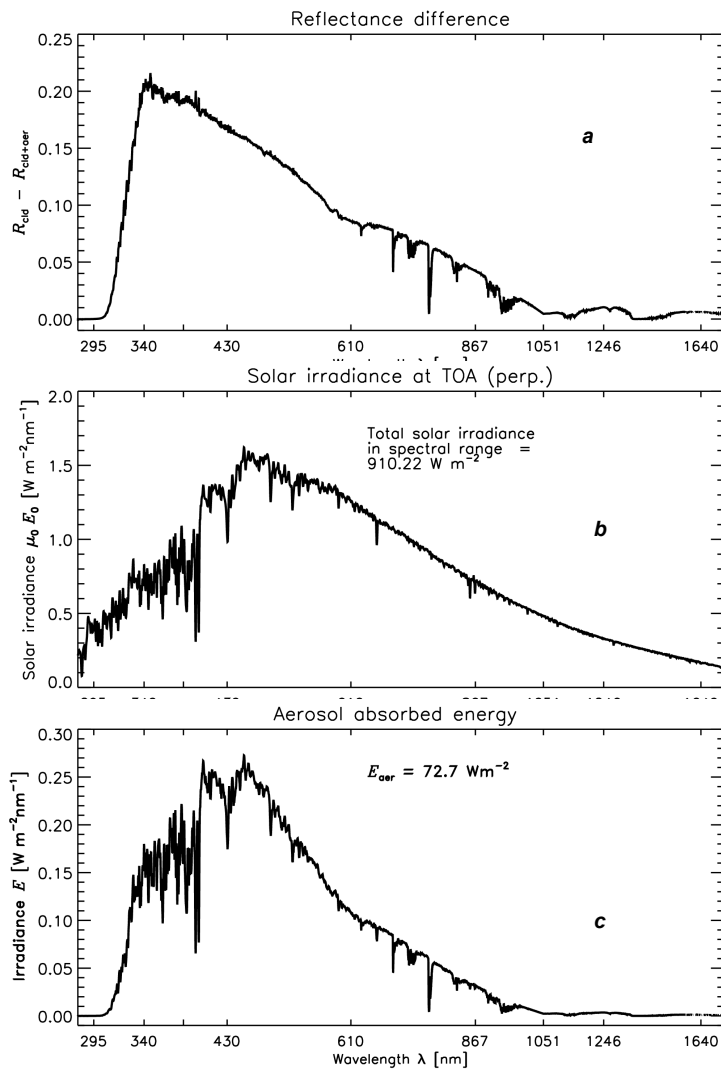
Figure 3: a) Difference between the measured polluted cloud reflectance spectrum and the modelled unpolluted cloud reflectance spectrum of the scene indicated by the black rectangle in Figure 1. b) Solar irradiance incident on the Earth's atmosphere for the given scene, proportional to a horizontal surface unit. c) Irradiance spectrum that is absorbed by the aerosols.

However, special care must be taken when retrieving these parameters in aerosol contaminated cloud scenes. Absorption by aerosols in the cloud retrieval bands can bias the retrieved cloud parameters, which is relevant in the current context. Therefore, the cloud parameters are retrieved as far in the infrared as possible, where the aerosol optical thickness becomes negligible.

With the retrieved cloud and scene parameters a reflectance spectrum can be simulated for an aerosol-unpolluted cloud scene. This reflectance spectrum can be compared with the measured reflectance and differences between the spectra (in the UV) can be attributed directly to aerosol absorption. With this method the aerosol direct effect can be determined for any water cloud scene for which the reflectance spectrum is measured in the solar spectral range.

REFERENCES

Ahmad, Z., Bhartia, P., and Krotkov, N. (2004) Spectral properties of backscatterd uv radiation in cloudy atmospheres. *J. Geoph. Res.*, **109**.

Coddington, O. M., Pilewskie, P., Redemann, J., Platnick, S., Russell, P. B., Schmidt, K. S., Gore, W. J., Livingston, J., Wind, G., and Vukicevic, T. (2010) Examining the impact of overlying aerosols on the retrieval of cloud optical properties from passive remote sensing. *J. Geoph. Res.*, **115**.

De Graaf, M., Stammes, P., Torres, O., and Koelemeijer, R. B. A. (2005) Absorbing Aerosol Index: Sensitivity Analysis, application to GOME and comparison with TOMS. *J. Geophys. Res.*, **110**.

De Graaf, M. and Stammes, P. (2005) SCIAMACHY Absorbing Aerosol Index. Calibration issues and global results from 2002 – 2004. *Atmos. Chem. Phys.*, **5**, 3367–3389.

De Graaf, M., Stammes, P., and Aben, E. A. A. (2007) Analysis of reflectance spectra of UV-absorbing aerosol scenes measured by SCIAMACHY. *J. Geoph. Res..*, **112**.

De Haan, J. F., Bosma, P. B., and Hovenier, J. W. (1987) The adding method for multiple scattering calculations of polarized light. *Astron. Astrophys.*, **183**, 371–391.

Diner, D. J., et al. (2001) MISR aerosol optical depth retrievals over Southern Africa during the SAFARI-2000 dry season campaign. *Geoph. Res. Lett.*, **28**, 3127–3130.

Forster, P., et al. (2007) Contribution of working group I to the fourth assessment report of the intergovernmental panel on climate change. Solomon, S., Qin, D., Manning, M., Chen, Z., Marquis, M., Averyt, K., Tignor, M., and Miller, H. (eds.), *Climate Change 2007: The Physical Science Basis.*, p. 996, Cambridge Univ. Press, Cambridge, UK and New York, NY, USA.

Hauser, A., Oesch, D., Foppa, N., and Wunderle, S. (2005) NOAA AVHRR derived aerosol optical depth over land. *J. Geophys. Res.*, **110**.

Haywood, J. M., Osborne, S. R., and Abel, S. J. (2004) The effect of overlying absorbing aerosol layers on remote sensing retrievals of cloud effective radius and cloud optical depth. *Q. J. R. Meteorol. Soc.*, **130**, 779–800.

Herman, J. R., Bhartia, P. K., Torres, O., Hsu, C., Seftor, C., and Celarier, E. A. (1997) Global distributions of UV-absorbing aerosols from NIMBUS 7/TOMS data. *J. Geophys. Res.*, **102**, 16,911–16,922.

Kawamoto, K., Nakajima, T., and Nakajima, T. Y. (2001) A global determination of cloud microphysics with AVHRR remote sensing. *Journal of Climate*, **14**, 2054–2068.

King, M. D. (2003) Cloud and Aerosol Properties, Precipitable Water, and Profiles of Temperature and Water Vapor from MODIS. *IEEE Trans. Geosci. Remote Sens. *, **41**, 442–458.

Nakajima, T. and King, M. D. (1990) Determination of the Optical Thickness and Effective Particle Radius of Clouds from Reflected Solar Radiation Measurements: Part I: Theory. *J. Atmos. Sci*, **47**.

Platnick, S., King, M. D., Ackerman, S. A., Menzel, W. P., Baum, B. A., Riédi, J. C., and Frey, R. A. (2003) The MODIS Cloud Products: Algorithms and Examples From Terra. *IEEE Transactions on Geoscience and Remote Sensing*, **41**, 459–473.

Roebeling, R. A., Feijt, A. J., and Stammes, P. (2006) Cloud property retrievals for climate monitoring: Implications of differences between Spinning Enhanced Visible and Infrared Imager (SEVIRI) on METEOSAT-8 and Advanced Very High Resolution Radiometer (AVHRR) on NOAA-17. *J. Geoph. Res.*, **111**, 2054–2068.

Stammes, P. (2001) Spectral radiance modelling in the UV-visible range. Smith, W. and Timofeyev, Y. (eds.), *IRS 2000: Current problems in atmospheric radiation*, pp. 385–388, A. Deepak Publishing, Hampton (VA).

Stammes, P., Tilstra, L. G., Braak, R., de Graaf, M., and Aben, E. A. A. (2008) Estimate of solar radiative forcing by polluted clouds using OMI and SCIAMACHY satellite data. *Proceedings of the International Radiation Symposium (IRS 2008)*, pp. 577–580, Foz do Iguau, Brazil.

Tanré, D., Herman, M., and Kaufman, Y. J. (1996) Information on aerosol size distribution contained in solar reflected spectral radiances. *J. Geophys. Res.*,**101**, 19,043–19,060.

Torres, O., Bhartia, P. K., Herman, J. R., Ahmad, Z., and Gleason, J. (1998) Derivation of aerosol properties from satellite measurements of backscattered ultraviolet radiation: Theoretical basis. *J. Geophys. Res.*, **103**, 17,099–17,110.

Veefkind, J. P., de Leeuw, G., Stammes, P., and Koelemeijer, R. B. A. (2000) Regional Distribution of Aerosol over Land, Derived from ATSR-2 and GOME. *Remote Sens. Environ.*, **74**, 377–386.

Wang, P., Stammes, P., van der A, R., Pinardi, G., and van Roozendael, M. (2008) FRESCO+: an improved O2 A-band cloud retrieval algorithm for tropospheric trace gas retrievals. *Atmos. Chem Phys.*, **8**, 6565–6576.

Wilcox, E. M. (2011) Direct and semi-direct radiative forcing of smoke aerosols over clouds. *Atmos. Chem Phys. Disc.*, **11**, 20947–20972.

Yu, H., et al. (2006) A review of measurement-based assessments of the aerosol direct radiative effect and forcing. *Atmos. Chem. Phys.*, **6**, 613–666.